ISSN 1062-8738, Bulletin of the Russian Academy of Sciences: Physics, 2018, Vol. 82, No. 5, pp. 516–519. © Allerton Press, Inc., 2018.
Original Russian Text © I.N. Didenkulov, N.V. Pronchatov-Rubtsov, V.G. Pazukhin, 2018, published in Izvestiya Rossiiskoi Akademii Nauk, Seriya Fizicheskaya, 2018, Vol. 82, No. 5.

Nonlinear Acoustic Profiling of Liquid Flows

I. N. Didenkulov[a, b, *], N. V. Pronchatov-Rubtsov[b], and V. G. Pazukhin[b]

[a] *Institute of Applied Physics, Russian Academy of Sciences, Nizhny Novgorod, 603950 Russia*
[b] *Lobachevsky State University, Nizhny Novgorod, 603950 Russia*
**e-mail: din@appl.sci-nnov.ru*

Abstract—A means of nonlinear acoustic Doppler tomography is described and the results from its simulation are analyzed. The technique can be applied to the gas inclusions normally present in liquids. The distribution of the flow velocity can be reconstructed by making certain assumptions about the distribution of gas inclusions.

DOI: 10.3103/S1062873818050064

INTRODUCTION

Acoustic means are widely used in the diagnostics of different media, medicine, and engineering [1, 2]. The distribution of the flow velocity over a stream's cross section often needs to be measured, especially in oceanography, medical diagnosis, and pipeline engineering. Echolocation, which is based on the scattering of sound by particles in the liquid, is usually used for this. The Doppler frequency shift in the detected signal allows us to measure the distribution of the flow velocity over the distance corresponding to the delay times of the echo signal. The spatial resolution, which is determined by the pulse duration, should be much less than the characteristic transverse scale of the flow. High acoustic frequencies must therefore be used in echolocation.

This technique cannot be applied to multi-phase media with high sound absorption. The tomography (transmission) approach, which is based on the nonlinear transformation of acoustic waves in a bubbly liquid, can in this case be used. It is known that gas bubbles strongly scatter acoustic waves [2]. This property is used in different diagnostic means that allow us to detect bubbles and determine their concentration and size distribution [2, 3]. Specific gas bubbles, i.e., contrast agents [4], are used in medical ultrasonic diagnosis to enhance contrast in the acoustic imaging of single organs.

Nonlinear acoustic effects are used in the diagnostics of liquid media and biological tissues [3–6]. One means of nonlinear acoustic diagnostics is the excitation of a difference frequency [3, 7], which allows us not only to detect bubbles of different sizes but also to obtain images of bubbly objects [8]. If an observed object moves, there is a Doppler frequency shift at the difference frequency [9] that can be used in problems of nonlinear acoustic diagnostics [10]. Below, we analyze the possibilities of this method in the profiling of flows.

THE DOPPLER SPECTRUM AT A DIFFERENCE FREQUENCY

If a bubble interacts with two acoustic waves having frequencies ω_1 and ω_2, and amplitudes P_1 and P_2, respectively, the component at frequency $\Omega = \omega_1 - \omega_2$ appears in the scattering field. The value of scattered field P_Ω at the difference frequency is proportional to the product of the pump wave amplitudes [7]:

$$P_\Omega = -\rho_0 \Omega^2 V_\Omega / 4\pi r, \quad (1)$$

where

$$V_\Omega = 2\pi P_1 P_2 [\rho_0^2 R_0 \omega_1^2 (\omega_0^2 - \Omega^2 + i\mu\Omega^2)]^{-1}. \quad (2)$$

Here, V_Ω is the deviation of the bubble volume from equilibrium value $V_0 = 4\pi R_0^3/3$ during oscillations at frequency Ω; $\omega_0 = (3\gamma P_0/\rho_0 R_0^2)^{1/2}$ is the eigenfrequency of the bubble; γ is the gas constant; R_0 is the equilibrium radius of the bubble under static pressure P_0; ρ_0 is the density of the liquid; and μ is the damping coefficient of the bubble oscillations. Expression (2) is valid under condition $\Omega, \omega_0 \ll \omega_1, \omega_2$. It follows from (2) that the scattered field at the difference frequency displays resonant behavior. If there are many bubbles in the area where two primary pump beams intersect, the scattered field is therefore determined only by the resonance bubbles, for which $\Omega \approx \omega_0$.

If a bubble moves at velocity v, frequency Ω_r of the scattered signals will differ from Ω [9]:

$$\begin{aligned}\Omega_r &= \Omega - (v/c)[\omega_1 \cos\theta_1 - \omega_2 \cos\theta_2 - \Omega\cos\theta_3] \\ &\approx \Omega - (v/c)[\omega_1 \cos\theta_1 - \omega_2 \cos\theta_2].\end{aligned} \quad (3)$$

Here, c is the speed of sound; θ_1 and θ_2 are angles between directions of propagation of the pump waves and the velocity vector; and θ_3 is the angle between the direction of wave propagation at the difference frequency from the bubble to the detector and the velocity vector. It follows from (3) that the Doppler shift at the difference frequency is virtually independent of the difference frequency.

If the resonance bubbles move with different frequencies within the area where the pump beams intersect, each of them will have a different Doppler frequency shift, and a broad line will emerge in the spectrum of the scattered signal.

The Doppler spectrum thus depends on the distribution of the concentration of resonance bubbles over velocities within the area where the pump beams intersect. The spatial distribution of the resonance bubbles within this area can vary in the liquid flow. In a laminar flow inside a tube, the cross-section distribution of the resonance bubbles is determined by the distribution at the input to the flow and can either be the same or differ from it. In developed turbulent flows, there are forces that act on bubbles and form the cross-section distribution that matches the flow. Experimental examples are presented below, and the possibility of reconstructing the distribution of the flow velocity under certain conditions is demonstrated.

EXPERIMENT AND SIMULATION

In the first experiment, a flow of water was produced in a PVC tube with a diameter of 10 mm. The tube was put into a water bath, in which also two pump transmitters with frequencies f_1 and f_2 were also placed. The area where the beams intersected was around 31 cm from the transmitters and passed through the tube. The angles between the transmitter axes and the tube were $\theta_1 = 30°$ and $\theta_2 = 150°$. The signals at the difference frequency were detected using a Bruel&Kjaer 8103 hydrophone and were transmitted to an Agilent DSO-X 3034A digital oscilloscope after amplification. The signal processing included spectral analysis of the signal and the subsequent accumulation of its spectral power over 1 min. In each series of measurements, the velocity of the water flow in the tube was varied along with frequency f_1 in the range of 2.07–2.1 MHz, while frequency f_2 = 2.0 MHz and other parameters remained the same.

Figure 1 shows the spectral power density (SPD) of the received signal at difference frequency $\Omega/2\pi$ = 70 (a) and 100 kHz (b) for a mean laminar water flow velocity of 30 cm s^{-1} inside the tube. The characteristic peaks at the zero Doppler shift are governed by the response of resonant bubbles adhering to the tube wall. The wide peak on the right is governed by the variation in the velocities of the resonance bubbles moving in the flow. The signal amplitude at the resonance frequency is governed by the concentration of the resonance bubbles. Our results show that the distribution of the electrolysis bubbles over the radius is not uniform. At electrolysis voltage U_{el} = 80 V in particular, the number of bubbles with a resonance frequency of 100 kHz exceeds that of those with resonance at 70 kHz. The similarity between the spectrum shapes of moving bubbles is governed by the laminar flow at which the concentration distribution of bubbles of different sizes remains the same over the tube section.

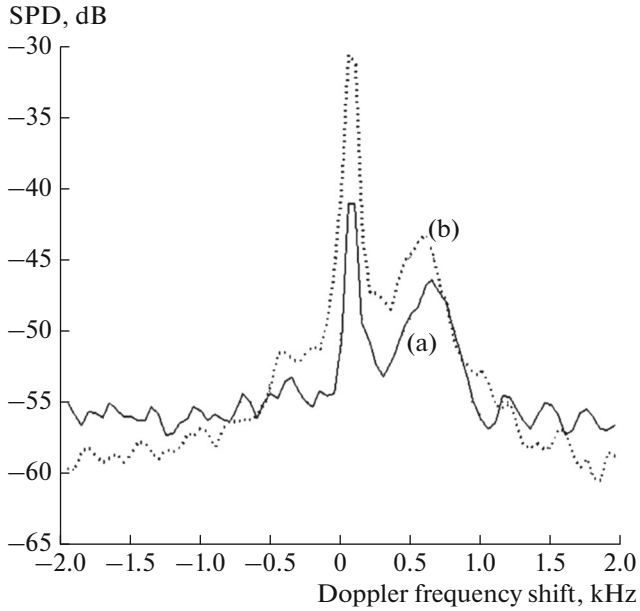

Fig. 1. Doppler spectrum at difference frequencies of (a) 70 and (b) 100 kHz for velocity v = 30 cm s^{-1} of water flow inside a tube.

The other experiment dealt with a developed turbulent flow. Its scheme is shown in Fig. 2. A submerged horizontal water jet in a pool escaped from a nozzle 1 cm in diameter at a depth of 41 cm. The velocity of the flow from the nozzle was of around 25 m s^{-1}. Two pump transmitters irradiated the submerged water jet at a distance of 60 cm from the nozzle, where the diameter of the jet was 11 cm. The size of the area where the pump beams intersected and the receiving system (a hydrophone and a semi-spherical reflector) exceeded the diameter of the jet. The frequencies of pump waves were f_1 = 1.1 MHz and f_2 = 1.0 MHz. The acoustic signal at difference frequency $F = f_1 - f_2$ = 100 kHz detected by the hydrophone and passed through a narrow-band amplifier was subjected to spectral analysis and accumulation.

We developed a numerical model of the Doppler spectrum using a cylindrical approximation of the distribution of the jet's velocity and the distribution of bubbles over its radius [11]:

$$v(\rho) = v_0 \exp(-\beta\rho^2),$$

$$n(\rho) = n_0 \exp(-2\beta\rho^2) \sim v^2,$$

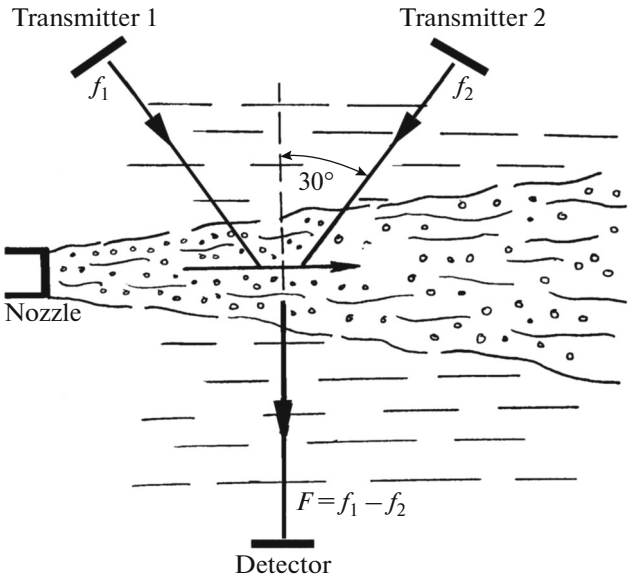

Fig. 2. Experimental setup with a submerged jet.

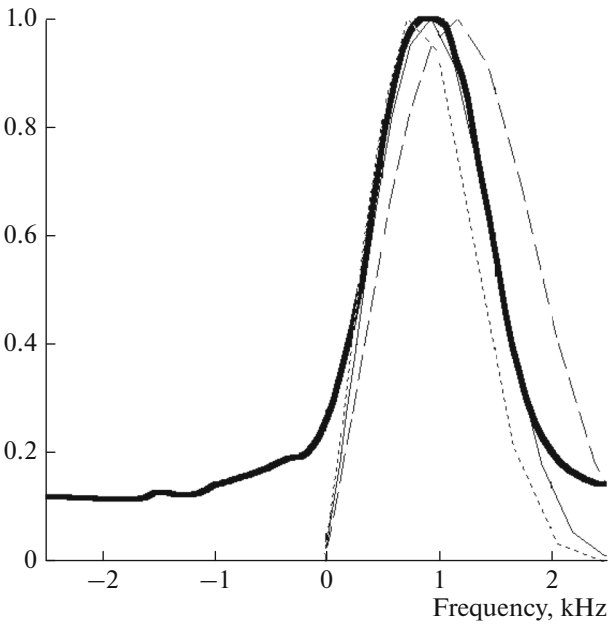

Fig. 4. Normalized Doppler spectra at the difference frequency: experiment (heavy line), theoretical model for different parameters (other lines).

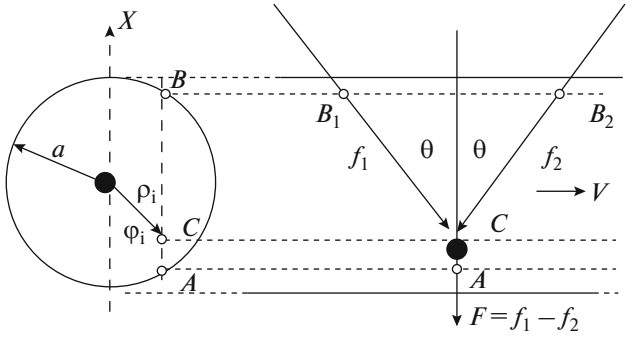

Fig. 3. Scheme of our theoretical model of a bubbly jet.

where V_0 and n_0 are the jet's velocity and the bubble concentration along the jet's axis, ρ is the radial coordinate, and β is a coefficient.

The calculation scheme is shown in Fig. 3 in two projections. Letters I_1 and I_2 mark the points at which the pump wave beams enter the cylindrical jet, and letter A marks the point at which the difference frequency exits the jet. Coordinates (ρ_i, φ_i) mark point C of beam intersection, where the pump waves are transformed into the difference frequency wave. The intensity of this wave is proportional to bubble concentration $n(\rho_i)$. According to formula (3), Doppler shift ΔF_i of the wave at the difference frequency emitted from the elementary volume at point C is

$$\Delta F_i \approx 2f_{1,2}(v_0/c)\sin\theta\exp(-\beta\rho_i^2).$$

Elementary intensity $\Delta I(\rho_i)$ associated with Doppler shift ΔF_i is

$$\Delta I(\rho_i) = \Delta I(\Delta F_i) \sim \exp\left(-2\beta\rho_i^2\right)$$
$$\times \int_0^{2\pi} d\varphi \left[\exp\left(-2\sigma_f \int_B^C n(\xi)d\xi - \sigma_F \int_C^A n(x)dx\right)\right],$$

where σ_f and σ_F are the cross sections of absorption by bubbles at the pump and difference frequencies (which can be determined from, e.g., the linear attenuation of sound in the jet [11]), and ξ is the coordinate along rays $B_{1,2}C$, which could exist.

The results from calculations of the normalized Doppler spectra at different parameters are shown in Fig. 4 by the fine, dashed, and dotted lines. The heavy line denotes the normalized Doppler spectrum of the signal at the difference frequency obtained experimentally. The best coincidence between the theoretical curve (thin line) is observed for parameters $v_0 = 3.2$ m s^{-1} and $\beta = 0.2$ cm^{-2}.

CONCLUSIONS

The results from our work demonstrate the possibility of profiling liquid flows using the nonlinear scattering of sound by gas bubbles at the difference frequency. The Doppler spectrum at the difference frequency carries information about the velocity distribution over the cross section of the liquid flow and the distribution of the bubble concentration. A priori data on the distribution of the bubble concen-

tration or independent measurements of their concentration allow us to reconstruct the distribution of the flow velocity.

ACKNOWLEDGMENTS

This work was supported by the Russian Science Foundation, project no. 14-12-00882.

REFERENCES

1. *Fizicheskie osnovy ul'trazvukovoi tekhnologii* (Physical Foundations of Ultrasonic Technology), Rozenberg, L.D., Ed., Moscow: Nauka, 1970.
2. Clay, C. and Medwin, H., *Acoustic Oceanography: Principle and Applications*, Wiley, 1977.
3. Leighton, T.G., *The Acoustic Bubble*, London: Academic, 1994.
4. Chereshneva, Yu.N and Mit'kov, V.V., *Ul'trazvuk. Diagn.*, 1999, no. 2, p. 6.
5. Ostrovsky, L.A., Gurbatov, S.N., and Didenkulov, J.N., *Acoust. Phys.*, 2005, vol. 51, p. 114.
6. Vilov, S.A., Didenkulov, I.N., Mart'yanov, A.I., et al., *Izv. Yuzhn. Fed. Univ. Tekh. Nauki*, 2014, no. 10, p. 145.
7. Sutin, A.M., Yoon, S.W., Kim, E.J., et al., *J. Acoust. Soc. Am.*, 1998, vol. 103, p. 2377.
8. Didenkulov, I.N., Kustov, L.M., Mart'yanov, A.I., and Pronchatov-Rubtsov, N.V., *Acoust. Phys.*, 2011, vol. 57, p. 241.
9. Didenkulov, I.N., Yoon, S.W., Sutin, A.M., et al., *J. Acoust. Soc. Am.*, 1999, vol. 106, p. 2431.
10. Didenkulov, I.N., Martyanov, A.I., and Pronchatov-Rubtsov, N.V., *Bull. Russ. Acad. Sci.: Phys.*, 2016, vol. 80, p. 1197.
11. Barkhatov, A.N., Gavrilenko, V.G., and Mart'yanov, A.I., *Akust. Zh.*, 1979, vol. 25, p. 32.

Translated by N. Podymova